

## Unique shape dependence in the coherent influence of signature on energies and $M1$ rates

G. B. Hagemann

*The Niels Bohr Institute, University of Copenhagen, Blegdamsvej 17, DK-2100 Copenhagen Ø, Denmark*

I. Hamamoto

*Department of Mathematical Physics, Lund Institute of Technology, P.O. Box 118, S-221 00 Lund, Sweden*

(Received 30 June 1989)

The relation between the signature splitting of energies and the signature dependence of  $M1$  transition matrix elements is investigated in connection with the deviation of nuclear shape from axial symmetry. The analysis of available experimental data on the signature dependences as well as the sign of  $E2/M1$  mixing ratio of the  $\Delta I = 1$  transition confirms our understanding of the structure of the rotational perturbation.

### I. INTRODUCTION

In high-spin nuclear physics, the energies of a variety of level sequences have been extensively measured as a function of spin ( $I$ ). However, it is known that energies may be interpreted in many ways and the interpretation is often not decisive in saying something about the structure of rotational perturbation. Electromagnetic moments can be used as a richer and more stringent source for studying the rotational perturbation. Recently, yrast spectroscopy experimental data on various electromagnetic moments with good accuracy have been accumulated.

The deviation of nuclear shape from axial symmetry is generally expected for high-spin states, though around the ground state of medium or heavy  $\beta$ -stable nuclei there has been no clear-cut evidence for the deviation. The recent development of the lifetime measurement of high-spin states provides  $B(E2: I \rightarrow I-2)$  values as a function of  $I$ . For example, the measurement<sup>1,2</sup> of <sup>158</sup>Er shows that, on the average, the  $B(E2)$  values of the yrast states decrease gradually as  $I$  increases up to 40. The decrease may well be interpreted as a result of triaxiality<sup>3</sup> ( $\gamma \rightarrow +60^\circ$ ). However, the decrease may also come from the change of  $\beta$  values, or a large difference of nuclear shape of the final state from that of the initial state, or a large shape fluctuation. Thus, in order to obtain a definite proof for the presence of the triaxial shape, it is desirable to find some of the phenomena which are incompatible with axially symmetric shape. Examples<sup>4</sup> of these phenomena which could be observed in odd- $A$  nuclei are signature inversion of quasiparticle Routhians  $E'(\alpha_u) < E'(\alpha_f)$ , the appreciable amount of signature dependence of  $B(E2: I \rightarrow I-1)$  values, and the inversion of signature dependence of  $B(M1)$  values,  $B(M1: \alpha_u I \rightarrow \alpha_f I-1) > B(M1: \alpha_f I+1 \rightarrow \alpha_u I)$ . Here,  $\alpha_f(\alpha_u)$  expresses the favored (unfavored) signature exponent and is equal to  $(\frac{1}{2})(-1)^{j-1/2} [(\frac{1}{2})(-1)^{j+1/2}]$  in a major shell which contains a "high- $j$ " orbit. Unfortunately, none of these phenomena have ever been clearly observed in odd- $A$  nuclei at the angular momentum

lower than that of the lowest band crossing, in which the interpretation of the nuclear structure is relatively simple.

In the present paper we examine the  $B(M1)$  values and their relation to the one-quasiparticle Routhians, choosing the unique-parity configurations of odd- $A$  nuclei in which the odd particle occupies a high- $j$  orbit (namely,  $i_{13/2}$  neutrons or  $h_{11/2}$  protons in the case of rare-earth nuclei). Furthermore, in the following we consider only the region of angular momentum lower than that of the first band crossing, since the nuclear structure in this region is well under control to say something definite. We have found that a variety of experimental data with good accuracy are already available to confirm our understanding of the structure of the rotational perturbation.

Taking an axially symmetric nuclear shape, in Sec. II we discuss the expected<sup>5</sup> vanishing  $B(M1: \alpha_u I \rightarrow \alpha_f I-1)$  values when the energies of the two states with different signatures are degenerate,  $E(\alpha_f, I+1) = E(\alpha_u, I)$ . The approximate degeneracy is, in fact, observed in some rare-earth nuclei such as <sup>165</sup>Yb. The  $E2/M1$  mixing ratio of the  $(\alpha_u, I) \rightarrow (\alpha_f, I-1)$  transition is expected to change sign, before and after the vanishing  $B(M1: \alpha_u I \rightarrow \alpha_f I-1)$  values. We present an analysis of the experimental data on Yb isotopes whose shape is consistent with axial symmetry at least for lighter members (see the analysis in Sec. III).

In Sec. III, taking a general triaxial shape, we discuss the relationship between the signature dependence of  $B(M1)$  values and the signature splitting of quasiparticle Routhians. In the application of this relationship to available experimental data, we have concluded that some  $h_{11/2}$  configurations of several odd- $Z$  rare-earth nuclei have a nuclear shape with an appreciable deviation from axial symmetry. Conclusions are given in Sec. IV.

### II. $M1$ TRANSITIONS IN THE CASE OF AXIALLY SYMMETRIC SHAPE

In Fig. 1 the level schemes of the positive-parity yrast sequence of some odd- $N$  Yb isotopes are shown. The positive parity in the present case means that the major com-

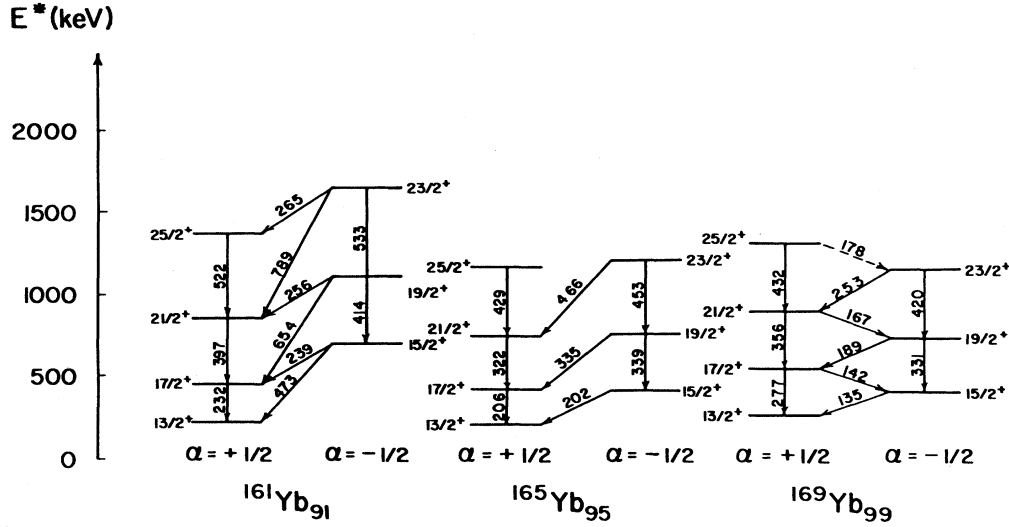


FIG. 1. Level scheme of positive-parity yrast sequence of three odd- $N$  Yb isotopes. Since the main component of the wave functions comes from the  $i_{13/2}$  orbit, the favored signature is  $\alpha_f = +\frac{1}{2}$ , while the unfavored signature is  $\alpha_u = -\frac{1}{2}$ . See the text for the discussion about the gradual change of the signature dependence of both energies and  $M1$  transition matrix elements, as the neutron number increases. Data are taken from Refs. 6, 7, and 8 for  $^{161}\text{Yb}$ ,  $^{165}\text{Yb}$ , and  $^{169}\text{Yb}$ , respectively.

ponent of the odd-neutron wave functions comes from the  $i_{13/2}$  orbit. It is known<sup>8</sup> that one observes the signature dependence of  $M1$  transitions which connect the favored signature ( $\alpha_f = +\frac{1}{2}$ ) band with the unfavored signature ( $\alpha_u = -\frac{1}{2}$ ) band. Namely, the  $B(M1: \alpha_f I + 1 \rightarrow \alpha_u I)$  value is larger than the  $B(M1: \alpha_u I \rightarrow \alpha_f I - 1)$  value. Specifically, the  $B(M1: \alpha_u I \rightarrow \alpha_f I - 1)$  values are extremely small in the case of  $^{165}\text{Yb}$ , in which the energy of the  $(\alpha_f, I + 1)$  state is near-

ly degenerate with that of the  $(\alpha_u, I)$  state. Assuming the collective nature for  $E2$  transitions, we estimate, for example, the upper limit of the  $B(M1: \alpha_u 19/2^+ \rightarrow \alpha_f 17/2^+)$  value<sup>9</sup> to be  $0.006\mu_N^2$ .

The  $B(M1)$  value, which is defined as,

$$B(M1: I_1 \rightarrow I_2) = \sum_{\mu M_2} |\langle I_2 M_2 | (M1)_\mu | I_1 M_1 \rangle|^2, \quad (1)$$

can be written as<sup>10</sup>

$$B(M1: I_1 \rightarrow I_2) = |\langle I_2, M_2 = I_2 | (M1)_{\mu = I_2 - I_1} | I_1, M_1 = I_1 \rangle|^2 \quad (2)$$

for  $I_1, I_2 \gg 1$ . The states in (2) with  $M = I$  may be taken<sup>11</sup> as cranked states by choosing the cranking axis as a quantization axis. In the case where the odd particle is in a high- $j$  orbit, the  $M1$  transition operator can be written to be proportional to the particle angular-momentum operator  $j_\mu$ . Namely, in the cranking model we have

$$(M1)_{\mu = \pm 1} \propto ij_y \mp j_z \quad (3)$$

taking the cranking axis as the  $x$  axis.

Now, if the intrinsic Hamiltonian is axially symmetric around the  $z$  axis, one obtains<sup>5</sup>

$$[H_{\text{cr}}, j_z] = [H_{\text{intr}} - \hbar\omega j_x, j_z] = \hbar\omega ij_y. \quad (4)$$

Taking the matrix element of the operator in (4) between the  $1qp$  states with the signature  $\alpha_u$  and  $\alpha_f$  we obtain

$$[E'(\alpha_u) - E'(\alpha_f)] \langle \alpha_u | j_z | \alpha_f \rangle = \hbar\omega \langle \alpha_u | ij_y | \alpha_f \rangle, \quad (5)$$

where  $E'(\alpha)$  expresses the quasiparticle Routhian

$$(H_{\text{intr}} - \hbar\omega j_x) |\alpha\rangle = E'(\alpha) |\alpha\rangle. \quad (6)$$

Expression (5) means

$$\langle \alpha_u | ij_y - j_z | \alpha_f \rangle = 0 \Leftrightarrow E'(\alpha_u) - E'(\alpha_f) = \hbar\omega. \quad (7)$$

Using the canonical relation

$$\hbar\omega = \frac{dE}{dI} \quad (8)$$

in Fig. 2 we illustrate what relation (7) means. We note

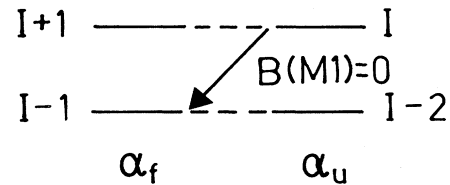


FIG. 2. Illustration of relation (7), which is obtained from the simplest version of the cranking model using an axially symmetric intrinsic shape and a single  $j$  shell.

that the situation of Fig. 2 is almost realized in the case of  $^{165}\text{Yb}$  (see Sec. III for the argument that the lighter Yb isotopes in Fig. 1 are consistent with the interpretation of having an axially-symmetric nuclear shape).

Here we note that the vanishing  $B(M1)$  value expressed in Fig. 2 is not the consequence of a perfect spin alignment. One also obtains the vanishing  $B(M1)$  value in the case of a perfect spin alignment, since the  $(\alpha_u, I)$  state has the core angular momentum  $R+2$  while the  $(\alpha_f, I-1)$  state has  $R$  and, thus, the  $M1$  transition operator cannot change the core angular momentum by 2. In order to illustrate the origin of the vanishing  $B(M1)$  value, in Fig. 3 we show the matrix elements of both  $ij_y$  and  $j_z$  as a function of cranking frequency, which are cal-

culated by using cranking-model wave functions. In the limit of very high cranking frequency, both matrix elements  $\langle \alpha_f | j_z | \alpha_u \rangle$  and  $\langle \alpha_f | ij_y | \alpha_u \rangle$  approach  $\frac{1}{2}\sqrt{2j}$  ( $=1.803$  for  $j = \frac{13}{2}$ ), irrespective of used parameters. It is seen that only for  $\frac{3}{2} \lesssim \Omega \lesssim \frac{5}{2}$  and for a particular value of  $\omega$  (pointed out by an arrow in the middle figure of Fig. 3) the matrix element of  $\langle \alpha_f | ij_y | \alpha_u \rangle$  becomes equal to that of  $\langle \alpha_f | j_z | \alpha_u \rangle$ , within the region of the cranking frequency lower than the lowest band-crossing frequency. At this particular value of  $\omega$  [ $= (0.049)\kappa$  for  $\lambda/\kappa = -0.68$ ], the relation between the energy-level scheme and the vanishing  $B(M1)$  value is expressed by Fig. 2, although the quasiparticle (for either  $\alpha_u$  or  $\alpha_f$ ) does not have a perfect spin alignment. The calculated spin alignment of the quasiparticle is 5.8 for  $\alpha_f$  and 4.3 for  $\alpha_u$ , while a perfect spin alignment means 6.5 for  $\alpha_f$  and 5.5 for  $\alpha_u$ .

The argument described in the above paragraph is based on cranking calculations. One might say that the cranking model is too crude to say something quantitatively about the transition matrix elements. However, one may notice that the analytically solvable model in which the  $j = \frac{1}{2}$  particle is coupled to a rotor produces exactly the situation expressed in Fig. 2. Furthermore, using the model in which a quasiparticle (with angular-momentum  $j$ ) is coupled to an axially symmetric rotor, we also conclude that if  $E(\alpha_f, I+1) = E(\alpha_u, I)$ , the  $B(M1: \alpha_u I \rightarrow \alpha_f I-1)$  value nearly vanishes. In fact, this is a special case of the relation, which will be discussed in detail in Sec. III.

Now, from expressions (3) and (5) and Fig. 3 we realize

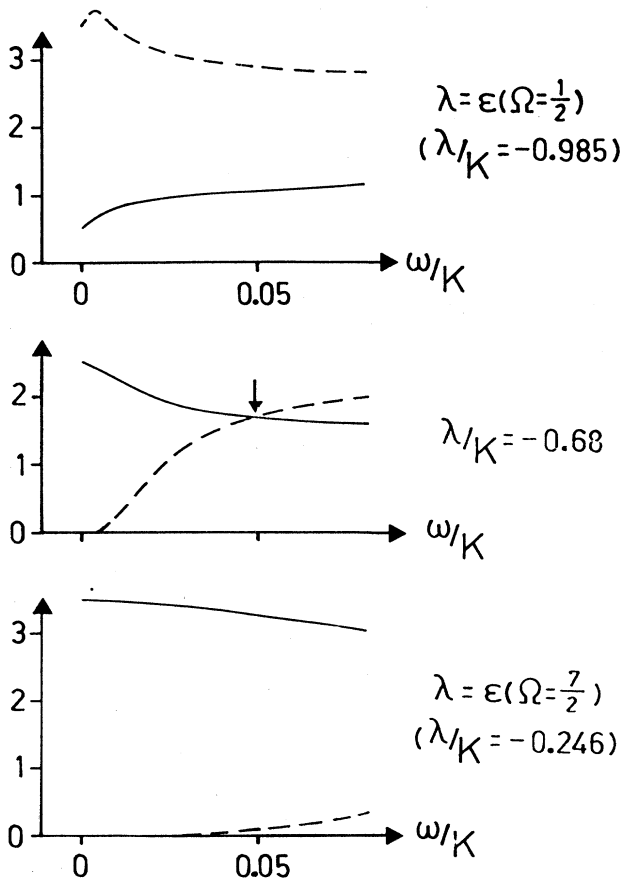


FIG. 3. Matrix elements  $\langle \alpha_f | j_z | \alpha_u \rangle$  and  $\langle \alpha_f | ij_y | \alpha_u \rangle$  expressed by solid lines and dashed lines, respectively, which are calculated by using the cranking-model wave functions of the yrast states as a function of the cranking frequency  $\omega$ . An axially-symmetric intrinsic shape is assumed and a single  $j = \frac{13}{2}$  shell is used. At  $\omega/\kappa = 0.049$  (pointed by an arrow) in the middle figure the situation illustrated in Fig. 2 is realized, although the spin alignments of the quasiparticles are still far away from the perfect alignment. See the text for details. The parameter  $\kappa$ , which is proportional to the  $Y_{20}$  deformation amplitude, is used as an energy unit (Ref. 12) for a single  $j$  shell and takes a value of  $2 \sim 3$  MeV. A pair-correlation parameter,  $\Delta/\kappa = 0.30$ , is used.

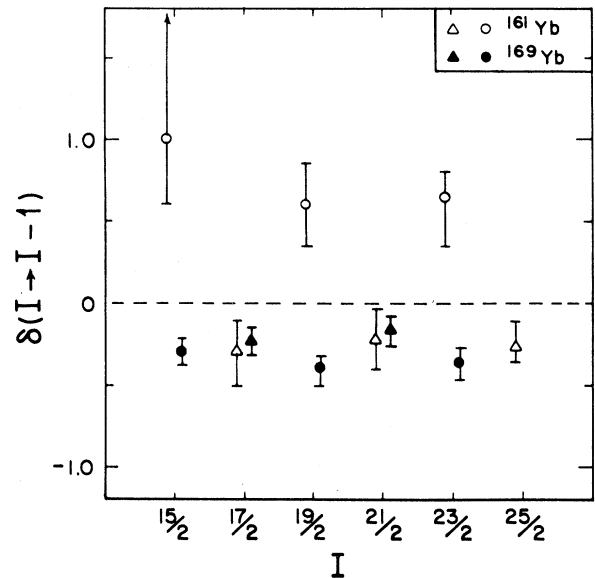


FIG. 4. Measured  $E2/M1$  mixing ratio of the  $I \rightarrow I-1$  transitions between the positive-parity yrast states in the nuclei  $^{161}\text{Yb}$  and  $^{169}\text{Yb}$ . Circles express the transitions  $(\alpha_u, I) \rightarrow (\alpha_f, I-1)$ , while triangles denote the transitions  $(\alpha_f, I) \rightarrow (\alpha_u, I-1)$ . References from which used data are given in Table I.

TABLE I. Analysis of  $E2/M1$  mixing ratio of the  $I \rightarrow I - 1$  transitions between positive-parity yrast states in the nuclei  $^{161}\text{Yb}$  and  $^{169}\text{Yb}$ .

$A$	$I$	$A_2$	$A_4$	$\alpha_2^a$	$\alpha_4^a$	$\delta$	Reference
161	$\frac{15}{2}$	1.54(85)	1.0(20)	0.35(12)	0.13(8)	1.0 (+15) (-4)	16
	$\frac{17}{2}^b$	0.23(25)	1.2(10)			-0.3 (2)	
	$\frac{19}{2}$	0.98(30)	-0.54(50)	0.48(13)	0.26(10)	0.6 (2) <sup>c</sup>	
	$\frac{21}{2}^b$	0.17(35)	0.04(56)			-0.22 (20)	
	$\frac{23}{2}$	0.61(25)	-0.12(30)	0.62(20)	0.40(15)	0.65(+15) (-30)	
	$\frac{25}{2}^b$	0.19(17)	-0.1(3)			-0.25(+15) (-10)	
169	$\frac{15}{2}$	-0.83(10)	0.17(17)	0.70(8)	0.29(10)	-0.30 (7)	8
	$\frac{17}{2}$	-0.72(16)	0.75(35)	0.74(8)	0.36(15)	-0.24 (10)	
	$\frac{19}{2}$	-0.96(10)	-0.13(13)	0.77(9)	0.43(15)	-0.40 (+7) (-10)	
	$\frac{21}{2}$	-0.60(16)	-0.10(10)	0.80(9)	0.48(17)	-0.17 (9)	
	$\frac{23}{2}$	-0.90(10)	0.30(10)	0.82(8)	0.53(15)	-0.36 (10)	

<sup>a</sup>From a smooth  $I$  dependence in the experimental attenuation coefficients,  $\alpha_2$  and  $\alpha_4$ , determined for the  $I \rightarrow I - 2$  transitions.

<sup>b</sup>Transition from  $I - 1 \rightarrow I$ .

<sup>c</sup>Results from a conversion electron measurement included.

that the  $E2/M1$  mixing ratio of the  $(\alpha_u, I) \rightleftharpoons (\alpha_f, I - 1)$  transition would have a different sign in the upper case in Fig. 3 from that in the lower case (and a different sign in the lower frequency than the arrow point from the higher frequency, in the middle case), since there is no reason to expect<sup>13,14</sup> that the matrix element  $\langle \alpha_u, I | E2 | \alpha_f, I - 1 \rangle$  should change sign in those two cases. In contrast, we expect that the  $E2/M1$  mixing ratio of the  $(\alpha_u, I) \leftrightarrow (\alpha_f, I + 1)$  transition always has a definite sign. Since experimental data with good accuracy are available on the positive-parity (i.e.,  $i_{13/2}$  orbits) yrast bands of the odd- $A$  Yb isotopes, we present, in the following, the analysis of the data.

Mixing ratios of several  $I \rightarrow I - 1$  transitions can be obtained in the Yb isotopes ranging from  $N=91$  to  $N=99$

from Refs. 15, 7, 8, and 16. For  $^{163}\text{Yb}$  the values of  $\delta$  are given in Ref. 15, which also contains a qualitative discussion of the signature dependence of the extracted  $M1$  transition rates for the neighboring odd- $A$  Yb isotopes. For  $^{161}\text{Yb}$  and  $^{165-169}\text{Yb}$ , the values of  $\delta$  have been extracted from the measurements of  $A_2$  and  $A_4$  published in Refs. 16, 7, and 8. The values used in the present analysis are given in Table I. For  $N=91$  and 99, the signature dependence in the energies is sufficiently large or small, respectively, so that we can extract values of the mixing ratio for both favored to unfavored and unfavored to favored  $\Delta I=1$  transitions in the spin range  $I = \frac{15}{2}$  to  $I = \frac{25}{2}$ . These are shown in Fig. 4, from which a clear distinction between the sign of  $\delta$  for the two types of transitions is demonstrated for the nucleus  $^{161}\text{Yb}$ , whereas for

TABLE II. Derivation of  $B(M1)$  values from branching ratios ( $\lambda$ ) and mixing ratio ( $\delta$ ) in positive-parity yrast states of odd- $A$  Yb isotopes. The energy of the transition  $I = \frac{19}{2} \rightarrow \frac{17}{2}$  is expressed by  $E1$ , while that of the transition  $I = \frac{19}{2} \rightarrow \frac{15}{2}$  is denoted by  $E2$ .

$A$	$E1$	$E2$	$\lambda$	$\delta$	$K$	$Q_0^a$	$\sqrt{B(M1, 19/2 \rightarrow 17/2)^b}$	Reference
161	653.9	414.5	1.4(2)	0.6 (2)	$\frac{1}{2}$	5.46	0.126(30)	16
163	483.6	370.3	4.33(50)	0.51 (12)	$\frac{3}{2}$	6.26	0.099(20)	15
165	335.2	339.1	4.13(50)	-1.6 (4)	$\frac{5}{2}$	6.90	-0.087(20)	7
167	236.5	314.2	1.86(20)	-0.55 (20)	$\frac{5}{2}$	7.39	-0.32(3)	7
169	189.1	330.9	3.17(40)	-0.40(+07) (-10)	$\frac{7}{2}$	7.58	-0.39(4)	8

<sup>a</sup>Average value of  $Q_0$  of neighboring even-even isotopes from Ref. 17.

<sup>b</sup>Sign given by the sign of  $\delta$ .

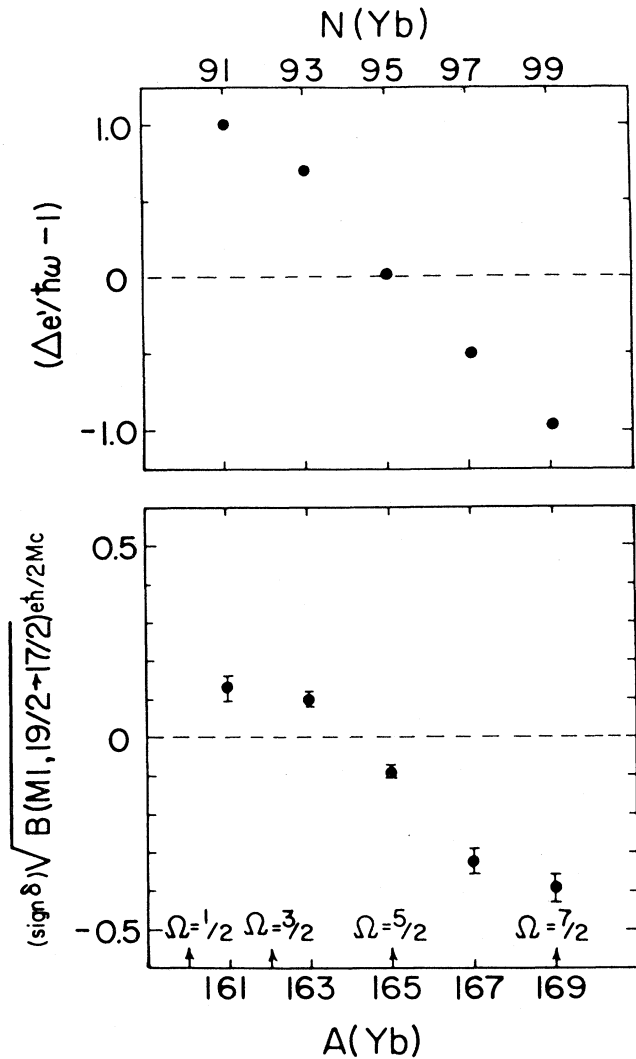


FIG. 5. Comparison between the  $M1$  ( $\alpha_u, I = \frac{19}{2}$ )  $\rightarrow$  ( $\alpha_f, I = \frac{17}{2}$ ) transition matrix elements and the signature dependence of the energies, which are extracted from available experimental data on odd- $N$  Yb isotopes. See the text for details. Assuming an axially symmetric intrinsic shape, the approximate positions of  $\Omega$  values are indicated in the lower figure. References from which used data are taken are given in Table II. The definition of  $\Delta e'$  and  $\hbar\omega$  is found in Eqs. (12) and (8), respectively.

$$[E'(\alpha_u) - E'(\alpha_f)] \langle \alpha_u | j_z | \alpha_f \rangle \approx \hbar\omega \langle \alpha_u | i j_y | \alpha_f \rangle - 2\sqrt{3} \frac{\kappa}{j(j+1)} \sin\gamma \{ \langle \alpha_u | j_x | \alpha_u \rangle + \langle \alpha_f | j_x | \alpha_f \rangle \} \langle \alpha_u | i j_y | \alpha_f \rangle. \quad (10)$$

Since the second term on the right-hand side (rhs) of (10) changes sign depending on the sign of  $\gamma$ , we may expect that, depending on the sign of  $\gamma$ , the relationship between the signature dependence of  $B(M1)$  values and the signature splitting of the quasiparticle Routhians would be shifted to a different direction. We will later confirm this

$^{169}\text{Yb}$  all the experimental mixing ratios have the same (negative) sign. The signs are in agreement with those obtained from the theoretical considerations using the  $i_{13/2}$  neutron configurations.

We now pursue the region of the change of sign by extracting the values of  $B(M1: \frac{19}{2} \rightarrow \frac{17}{2})$  from the experimental branching ratios, mixing ratios, and the values of  $B(E2: \frac{19}{2} \rightarrow \frac{17}{2})$  calculated assuming a transition quadrupole moment averaged between the two neighboring even-even Yb isotopes and the value of  $K$  necessary in the Clebsch-Gordan coefficient given in Table II. The square root of  $B(M1: \frac{19}{2} \rightarrow \frac{17}{2})$  values with the sign following the mixing ratio for the  $\frac{19}{2} \leftrightarrow \frac{17}{2}$  transition is presented in the lower part of Fig. 5 for the entire range of nuclei. This range includes Fermi levels corresponding to  $\Omega = \frac{1}{2}$  as well as  $\Omega = \frac{7}{2}$  as marked on the abscissa of Fig. 5.

The relationship between the signature splitting in Routhian  $\Delta e'$  and the size and sign of the  $(M1, \frac{19}{2} \rightarrow \frac{17}{2})$  matrix element is clearly demonstrated in the comparison of the two graphs in Fig. 5. In the upper part of Fig. 5 the value of the difference from unity of the relative signature splitting in Routhians  $\Delta e'/\hbar\omega$  is plotted for the same nuclei at  $I = \frac{19}{2}$ . In accordance with the expectations from the cranking expression<sup>18</sup> of Eqs. (3) and (7), the sign of the  $M1$  matrix element changes close to the situation with total degeneracy in which  $\Delta e'/\hbar\omega$  equals one.

### III. RELATIONSHIP BETWEEN THE SIGNATURE DEPENDENCE OF $B(M1)$ VALUES AND THE SIGNATURE SPLITTING OF ROUTHIAN IN TRIAXIAL SHAPE

In the cranking model with quasiparticles in a  $j$  shell relation (4) is straightforwardly extended to the case of a triaxial shape (i.e.,  $\gamma \neq 0$ ) namely,

$$[H_{cr, j_z}] = \hbar\omega i j_y - 2\sqrt{3} \frac{\kappa}{j(j+1)} \sin\gamma (i j_y j_x + j_x i j_y), \quad (9)$$

where  $\kappa$  is the energy unit for a single  $j$  shell used in Ref. 12. Then we obtain

expectation using a particle-rotor model (compare Figs. 8 and 10). However, a literal use of the cranking-model formula [Eq. (3)] together with Eq. (10) leads to the results which are pretty different from those in Figs. 8 and 10. The differences comes from the fact that for smaller triaxiality and lower rotational frequency the one-

dimensional cranking is a poor approximation to the description of a quantum state with a given angular momentum. In the case of  $\gamma = +15^\circ$  the cranking-model result is qualitatively very different from Fig. 10.

In order to extract information on the deviation of the nuclear shape from axial symmetry using the signature dependence of both  $B(M1)$  values and Routhians, we return to the relation in the case of axially symmetric shape [Eq. (5)]. From (5) we obtain

$$\frac{B(M1:\alpha_u I \rightarrow \alpha_f I - 1)}{B(M1:\alpha_f I + 1 \rightarrow \alpha_u I)} = \left[ \frac{\Delta e' - \hbar\omega}{\Delta e' + \hbar\omega} \right]^2, \quad (11)$$

where

$$\Delta e' \equiv E'(\alpha_u, \omega) - E'(\alpha_f, \omega). \quad (12)$$

Here we write explicitly the dependence of quasiparticle Routhians on the cranking frequency. The vanishing  $B(M1)$  value discussed in Sec. II is a special case of relation (11). Namely, in the case of  $\Delta e' = \hbar\omega$ , the  $B(M1:\alpha_u, I \rightarrow \alpha_f, I - 1)$  value vanishes according to (11). For an axially-symmetric shape relation (11) is exact (a) in the cranking model for any cranking frequency  $\omega$ , (b) in the particle-rotor model with a particle in a  $j = \frac{1}{2}$  shell for  $I \gg 1$ , when the quantity  $\omega$  is defined by (8), and (c) in the deformation-aligned band (i.e., in the case that  $K$  is a good quantum number) with a particle in a  $j$  shell for  $I \gg 1$ , defining  $\omega$  by (8).

We rewrite (11) in the form<sup>19</sup>

$$\frac{\Delta B(M1)}{B(M1)_{av}} = \frac{4(\Delta e')(\hbar\omega)}{(\Delta e')^2 + (\hbar\omega)^2}, \quad (13)$$

where

$$\Delta B(M1) \equiv B(M1:\alpha_f \rightarrow \alpha_u) - B(M1:\alpha_u \rightarrow \alpha_f) \quad (14)$$

and

$$B(M1)_{av} \equiv \frac{1}{2} \{ B(M1:\alpha_f \rightarrow \alpha_u) + B(M1:\alpha_u \rightarrow \alpha_f) \}. \quad (15)$$

In order to show the validity of relation (13) for a rotational band with an axially-symmetric intrinsic shape, in Fig. 6 we compare the quantity on the left-hand side (lhs) with the rhs quantity of (13), both of which are calculated by using a particle-rotor model in which one quasiparticle occupies a  $j = \frac{11}{2}$  shell. Having the calculated energies ( $E$ ) as a function of  $I$ , the rotational frequencies are calculated by using Eq. (8), while the Routhians ( $E'$ ) used in the definition of  $\Delta e'$  in (12) are defined as  $(E - \hbar\omega I)$ . The comparison was made by using the calculated energies and  $B(M1)$  values around  $I = \frac{19}{2}$ . It is seen that for the axially-symmetric shape, relation (13) holds with good accuracy. In particular, we remark that for  $\Delta e' = \hbar\omega$  (i.e., the case shown in Fig. 2) the quantity on the rhs of (13) is equal to +2 and, then, from Fig. 6 the lhs quantity is seen to be equal to +2 with very good accuracy.

In Fig. 7 we choose several odd- $N$  (in which the odd neutron is in the  $i_{13/2}$  orbit) and odd- $Z$  (in which the odd proton is in the  $h_{11/2}$  orbit) nuclei, and compare both sides of expression (13) which are estimated by using the

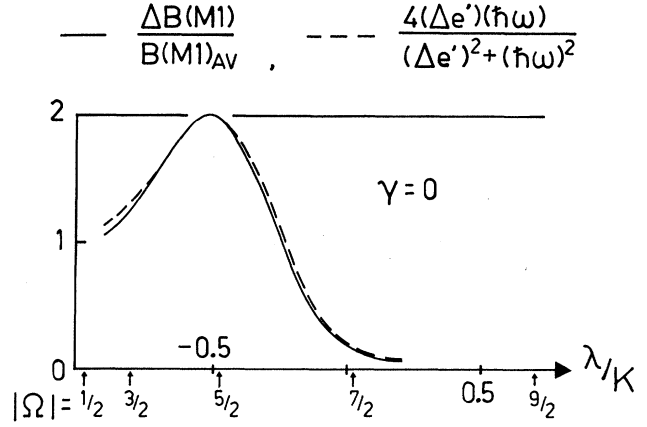


FIG. 6. Comparison between the quantity of the lhs (solid line) and that of the rhs (dashed line) in (13), both of which are calculated by using a particle-rotor model (Ref. 14) in which one quasiparticle occupies a  $j = \frac{11}{2}$  shell. The comparison was made by using the calculated energies and  $B(M1)$  values around  $I = \frac{19}{2}$ . Used parameters are  $\Delta/\kappa = 0.30$ ,  $g_l = 1.0$ ,  $g_s = +3.91$ ,  $g_R = 0.40$ , and  $\kappa J_0/\hbar^2 = 75$ . These relative values are hardly affected by the used values of  $g$  factors.

observed energies and  $B(M1)$  values. The estimate of the rhs of (13) is done exactly in the same way as is done in plotting Fig. 6, except using the observed energies ( $E$ ). We remark that the quantity on the lhs of (13) is constructed so that one may use the measured ratio  $B(M1:I \rightarrow I - 1)/B(E2:I \rightarrow I - 2)$  instead of the  $B(M1:I \rightarrow I - 1)$  values themselves, when the  $B(E2:I \rightarrow I - 2)$  values have a smooth dependence<sup>26</sup> on  $I$  and do not appreciably depend on the signature. From Fig. 7 it is observed that in the lighter Yb isotopes relation (13) holds with good accuracy, while in some of the odd- $Z$  nuclei the relation is drastically violated. We note that the quantity on either side of (13) can, in principle,

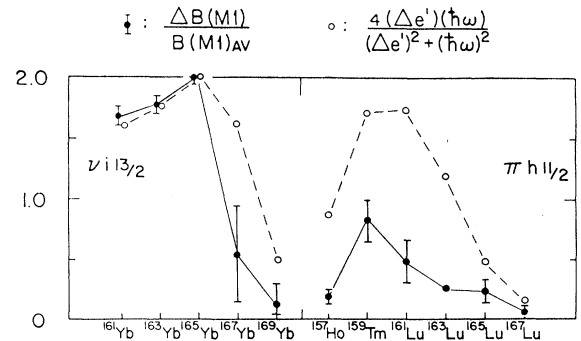


FIG. 7. Comparison between the quantity of the lhs (filled circles) and that of the rhs (open circles) in (13), both of which are estimated by using experimental data. The comparison was made by choosing the data around  $I = \frac{19}{2}$ . Experimental data are taken from Refs. 16, 15, 7, 7, 8, 20, 21, 22, 23, 24, and 25 for  $^{161}\text{Yb}$ ,  $^{163}\text{Yb}$ ,  $^{165}\text{Yb}$ ,  $^{167}\text{Yb}$ ,  $^{169}\text{Yb}$ ,  $^{157}\text{Ho}$ ,  $^{159}\text{Tm}$ ,  $^{161}\text{Lu}$ ,  $^{163}\text{Lu}$ ,  $^{165}\text{Lu}$ , and  $^{167}\text{Lu}$ , respectively.

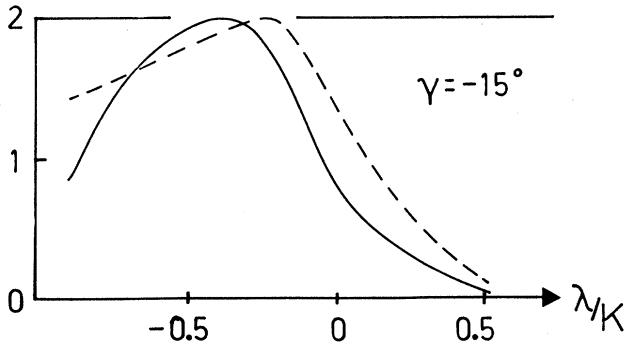


FIG. 8. The same as in Fig. 6, except for  $\gamma = -15^\circ$ . The ratio of the three moments of inertia for a given  $\gamma$  value is taken to be equal to that of the hydrodynamic moments of inertia.

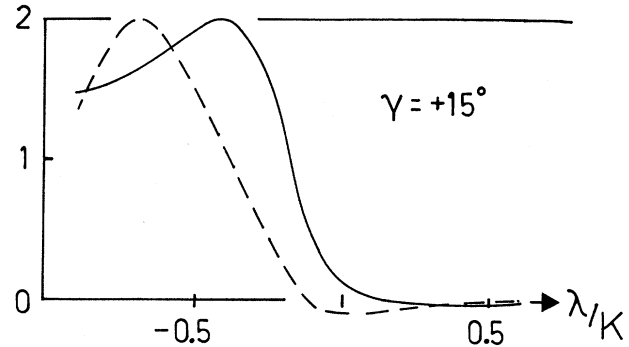


FIG. 10. The same as in Fig. 6, except for  $\gamma = +15^\circ$ .

take a value between  $-2$  and  $+2$ .

In order to understand the comparison shown in Fig. 7 for odd- $Z$  nuclei, in Figs. 8 and 9 we plot the quantities on both sides of (13), which are calculated by using a particle-rotor model with  $\gamma = -15^\circ$  and  $-25^\circ$ . We note that the  $h_{11/2}$  proton shell filling in the nuclei  $^{67}\text{Ho}$ ,  $^{69}\text{Tm}$ , and  $^{71}\text{Lu}$  corresponds to the region  $0 \lesssim \lambda/\kappa \lesssim 0.6$ . Though the very quantitative numbers in Figs. 8 and 9 depend on the used parameters in the particle-rotor calculation, the comparison of measured quantities in Fig. 7 with the calculated quantities in Figs. 8 and 9 seems to

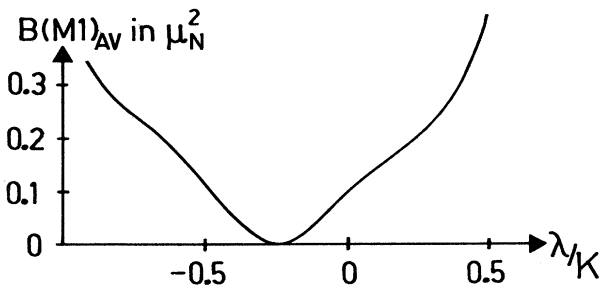
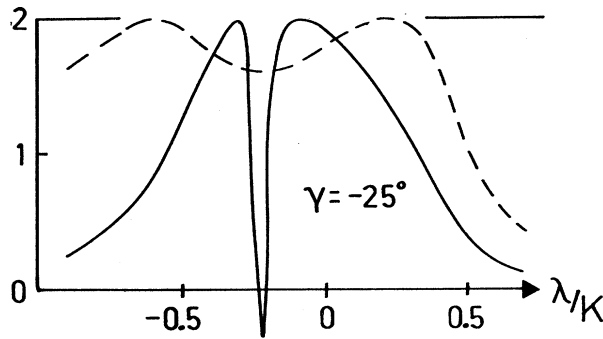


FIG. 9. The upper part is the same as in Fig. 8, except for  $\gamma = -25^\circ$ . The lower part shows the calculated  $B(M1)_{av}$  values defined in (15), in order to demonstrate the peculiarity of the nature of the calculated yrast (unfavored signature) states in the region of  $-0.4 \lesssim \lambda/\kappa \lesssim -0.1$ .

indicate that the nuclei  $^{157}\text{Ho}$ ,  $^{159}\text{Tm}$ , and the lighter isotopes of Lu have an appreciable amount of deviation from the axially symmetric shape and are consistent with the shape of  $-15^\circ \lesssim \gamma \lesssim -25^\circ$ . For reference, in Fig. 10 we show the quantities in (13) calculated by using the particle-rotor model with  $\gamma = +15^\circ$ , in which the moments of inertia for the positive  $\gamma$  value are defined in the same way as in Ref. 14.

The  $\gamma$  values concluded from the above comparison are consistent with the  $\gamma$  values which are previously obtained from theoretical considerations.<sup>27,28</sup> Namely, in the  $i_{13/2}$  neutron configuration of the lighter Yb isotopes the Fermi level lies around the lower part of the  $i_{13/2}$  shell and, thus, the aligned  $i_{13/2}$  neutron prefers an approximately axially symmetric shape. In contrast, the  $h_{11/2}$  protons in the nuclei with  $Z = 67 \sim 71$  fill in the  $h_{11/2}$  shell more than half and, thus, the aligned  $h_{11/2}$  proton may prefer a shape with an appreciable negative  $\gamma$  value.

We make a comment on the "peculiar" behavior of the  $\Delta B(M1)/B(M1)_{av}$  values in Fig. 9 in the region of  $-0.4 \lesssim \lambda/\kappa \lesssim -0.1$ . In this region a unique way of rotation<sup>29</sup> in unfavored signature states, which is clearly different from the cranking picture, is realized for some triaxial intrinsic shapes, if a definite direction of the particle angular momentum ( $j$ ) is so much favored by the intrinsic field. The way of rotation is, in fact, easily recognized by very small  $B(M1)$  values. The smallness comes from the fact that the vector  $j$  does not really change its direction in the unfavored states from the one in the favored states. In the lower part of Fig. 9 we show, for reference, the calculated  $B(M1)_{av}$  values. The idealistic case ( $\lambda/\kappa = 0.0$  and  $\gamma = -30^\circ$ ) of this unique way of rotation is explained in Ref. 29.

#### IV. CONCLUSIONS

Choosing the unique-parity configurations of odd- $A$  nuclei in which the odd particle occupies a high- $j$  orbit we have shown that for an axially-symmetric shape one obtains, with very good accuracy, a definite relation [expressed by (13)] between the signature splitting of energies and the signature dependence of  $B(M1: I \rightarrow I-1)$  values. As a special case of the relation, the  $M1$  transi-

tion matrix element between the  $(\alpha_u, I)$  state and the  $(\alpha_f, I-1)$  state is expected to vanish when the  $(\alpha_f, I+1)$  state is degenerate with the  $(\alpha_u, I)$  state. Before and after the degeneracy occurs, the  $E2/M1$  mixing ratio of the  $(\alpha_u, I) \leftrightarrow (\alpha_f, I-1)$  transition is expected to change its sign, while the mixing ratio of the  $(\alpha_f, I+1) \leftrightarrow (\alpha_u, I)$  transition will always have a definite sign. We have confirmed all these expectations by analyzing the available experimental data on the positive-parity yrast level sequence of odd- $A$  Yb isotopes ( $N = 161-169$ ).

For axially-asymmetric shapes the particle-rotor calculations show that there exists a unique shape ( $\gamma$ ) dependence in the coherent influence of signature on energies

and  $M1$  transition matrix elements.

Comparing the quantities on both sides of expression (13) which are calculated by using experimental data, one may therefore obtain an estimate of both the sign of the triaxiality parameter  $\gamma$  and the amount of deviation of the nuclear shape from axial symmetry. The analysis of available experimental data indicates that the negative-parity yrast level sequences in the nuclei  $^{157}\text{Ho}$ ,  $^{159}\text{Tm}$ , and the lighter isotopes of Lu are consistent with an appreciable amount of triaxiality such as  $\gamma = -15^\circ \sim -25^\circ$ .

Stimulating discussions with F. Dönau, B. Mottelson, W. Nazarewicz, and C.-H. Yu are highly acknowledged.

<sup>1</sup>M. Oshima, N. R. Johnson, F. K. McGowan, C. Baktash, I. Y. Lee, Y. Schutz, R. V. Ribas, and J. C. Wells, *Phys. Rev. C* **33**, 1988 (1986).

<sup>2</sup>E. M. Beck, H. Hübel, R. M. Diamond, J. C. Bacelar, M. A. Deleplanque, K. H. Maier, R. J. McDonald, F. S. Stephens, and P. O. Tjøm, *Phys. Lett. B* **215**, 624 (1988).

<sup>3</sup>We use the Lund convention of the  $\gamma$  variable; G. Andersson *et al.*, *Nucl. Phys. A* **268**, 205 (1976).

<sup>4</sup>For example, see I. Hamamoto, in Proceedings of the Workshop on Microscopic Models in Nuclear Structure Physics, Oak Ridge, 1988 (World Scientific, Singapore, to be published), p. 173.

<sup>5</sup>I. Hamamoto, *Phys. Lett.* **102B**, 225 (1981); **106B**, 281 (1981).

<sup>6</sup>L. L. Riedinger, *Nucl. Phys. A* **347**, 141 (1980).

<sup>7</sup>N. Roy, S. Jönsson, H. Ryde, W. Walus, J. J. Gaardhøje, J. D. Garrett, G. B. Hagemann, and B. Herskind, *Nucl. Phys. A* **382**, 125 (1982).

<sup>8</sup>E. Selin, S. A. Hjorth, and H. Ryde, *Phys. Scr.* **2**, 181 (1970).

<sup>9</sup>The matrix element given in Table II and Fig. 5 extracted using experimental mixing ratios corresponds to a slightly higher value.

<sup>10</sup>E. R. Marshalek, *Phys. Rev. C* **11**, 1426 (1975); *Nucl. Phys. A* **266**, 317 (1976); A. Bohr and B. R. Mottelson, *Nuclear Structure* (Benjamin, New York, 1975), Vol. 2.

<sup>11</sup>I. Hamamoto and H. Sagawa, *Nucl. Phys. A* **327**, 99 (1979).

<sup>12</sup>I. Hamamoto, *Nucl. Phys. A* **271**, 15 (1976).

<sup>13</sup>P. Arve, *Phys. Lett.* **197B**, 307 (1987).

<sup>14</sup>I. Hamamoto and B. Mottelson, *Phys. Lett.* **132B**, 7 (1983).

<sup>15</sup>J. Kownacki, J. D. Garrett, J. J. Gaardhøje, G. B. Hagemann, B. Herskind, S. Jönsson, N. Roy, H. Ryde, and W. Walus, *Nucl. Phys. A* **394**, 269 (1983).

<sup>16</sup>J. J. Gaardhøje, Ph.D thesis, University of Copenhagen, 1980.

<sup>17</sup>S. Raman, C. H. Malarkey, W. T. Milner, C. W. Nestor, Jr., and P. H. Stelson, *At. Data Nucl. Data Tables* **36**, 1 (1987).

<sup>18</sup>An expression for an axially symmetric shape, which originates from an idea of using cranking-model wave functions in the expression of a particle rotor model is found in F. Dönau,

*Nucl. Phys. A* **471**, 469 (1987).

<sup>19</sup>Relation (13) was used in the analysis of data in G. B. Hagemann, R. Chapman, P. Frandsen, A. R. Mokhtar, M. Riley, J. Simpson, and C.-H. Yu, in Proceedings of the International Conference on Nuclear Structure through Static and Dynamic Moments, Melbourne, Australia, 1987, p. 313.

<sup>20</sup>D. C. Radford *et al.*, Chalk River Nuclear Laboratory Annual Report, 1988 (unpublished).

<sup>21</sup>J. Gascon, P. Taras, D. C. Radford, D. Ward, H. R. Andrews, and F. Banville, *Nucl. Phys. A* **467**, 539 (1987).

<sup>22</sup>C.-H. Yu, M. Riley, J. D. Garrett, G. B. Hagemann, J. Simpson, P. D. Forsyth, A. R. Mokhtar, J. D. Morrison, B. M. Nyako, J. F. Sharpey-Schafer, and R. Wyss, *Nucl. Phys. A* **489**, 477 (1988).

<sup>23</sup>K. Honkanen *et al.*, Proceedings of the 1986 ACS Meeting.

<sup>24</sup>S. Jönsson, J. Lyttkens, L. Carlen, N. Roy, H. Ryde, W. Walus, J. Kownacki, G. B. Hagemann, B. Herskind, J. D. Garrett, and P. O. Tjøm, *Nucl. Phys. A* **422**, 397 (1984); P. Frandsen, R. Chapman, J. D. Garrett, G. B. Hagemann, B. Herskind, C.-H. Yu, K. Schiffer, D. Clarke, F. Khazaie, J. C. Lisle, J. N. Mo, L. Carlen, P. Ekström, and H. Ryde, *ibid.* **A489**, 508 (1988).

<sup>25</sup>C.-H. Yu, J. M. Espino, K. Furuno, P. Frandsen, J. D. Garrett, G. B. Hagemann, R. Chapman, D. Clarke, F. Khazaie, J. C. Lisle, and J. N. Mo, The Niels Bohr Institute and Nordita, Activity Report 1988, p. 59; C. H. Yu, J. M. Espino, K. Furuno, J. D. Garrett, G. B. Hagemann, R. Chapman, D. Clarke, F. Khazaie, J. C. Lisle, J. N. Mo, M. Bergström, L. Carlen, P. Ekström, J. Lyttkens-Linden, and H. Ryde, *Nucl. Phys.* (to be published).

<sup>26</sup>The squared Clebsch-Gordan coefficients change about 10% only in the angular-momentum range  $I = \frac{17}{2} - \frac{23}{2}$  for a realistic value of  $K \sim \frac{3}{2}$ .

<sup>27</sup>S. Frauendorf and F. R. May, *Phys. Lett.* **125B**, 245 (1983).

<sup>28</sup>I. Hamamoto and B. Mottelson, *Phys. Lett.* **127B**, 281 (1983).

<sup>29</sup>I. Hamamoto, *Phys. Lett. B* **193**, 399 (1987).